

ARL LIBRARY (APG)



5 0592 01018536 6

ADA 123 792

MEMORANDUM REPORT ARBRL-MR-03238

A SHORT-BARRELLED 105MM HOWITZER
FOR INTERIOR BALLISTIC STUDIES

Carl R. Ruth
James W. Evans

January 1983



US ARMY ARMAMENT RESEARCH AND DEVELOPMENT COMMAND
BALLISTIC RESEARCH LABORATORY
ABERDEEN PROVING GROUND, MARYLAND

Approved for public release; distribution unlimited.

Destroy this report when it is no longer needed.
Do not return it to the originator.

Secondary distribution of this report is prohibited.

Additional copies of this report may be obtained
from the National Technical Information Service,
U. S. Department of Commerce, Springfield, Virginia
22161.

The findings in this report are not to be construed as
an official Department of the Army position, unless
so designated by other authorized documents.

*The use of trade names or manufacturers' names in this report
does not constitute endorsement of any commercial product.*

UNCLASSIFIED

SECURITY CLASSIFICATION OF THIS PAGE (When Data Entered)

REPORT DOCUMENTATION PAGE		READ INSTRUCTIONS BEFORE COMPLETING FORM
1. REPORT NUMBER Memorandum Report ARBRL-MR-03238	2. GOVT ACCESSION NO.	3. RECIPIENT'S CATALOG NUMBER
4. TITLE (and Subtitle) A Short-Barrelled 105-mm Howitzer for Interior Ballistic Studies		5. TYPE OF REPORT & PERIOD COVERED Memorandum Report
		6. PERFORMING ORG. REPORT NUMBER
7. AUTHOR(s) Carl R. Ruth and James W. Evans		8. CONTRACT OR GRANT NUMBER(s)
9. PERFORMING ORGANIZATION NAME AND ADDRESS US Army Ballistic Research Laboratory ATTN: DRDAR-BLI Aberdeen Proving Ground, MD 21005		10. PROGRAM ELEMENT, PROJECT, TASK AREA & WORK UNIT NUMBERS 1L162618AH80
11. CONTROLLING OFFICE NAME AND ADDRESS US Army Armament Research & Development Command US Army Ballistic Research Laboratory (DRDAR-BL) Aberdeen Proving Ground, MD 21005		12. REPORT DATE January 1983
		13. NUMBER OF PAGES 41
14. MONITORING AGENCY NAME & ADDRESS (if different from Controlling Office)		15. SECURITY CLASS. (of this report) UNCLASSIFIED
		15a. DECLASSIFICATION/DOWNGRADING SCHEDULE
16. DISTRIBUTION STATEMENT (of this Report) Approved for public release; distribution unlimited.		
17. DISTRIBUTION STATEMENT (of the abstract entered in Block 20, if different from Report) TECHNICAL REPORTS SECTION STINFO BRANCH BLDG. 305		
18. SUPPLEMENTARY NOTES		
19. KEY WORDS (Continue on reverse side if necessary and identify by block number) Interior Ballistics Resistive Pressure Howitzers Accelerometers On-board Instrumentation		
20. ABSTRACT (Continue on reverse side if necessary and identify by block number) jaf Knowledge of the resistance to projectile motion is a requirement for interior ballistic simulation models. The behavior of the projectile during the engraving process is of particular interest. This need has prompted the development of techniques designed to provide detailed measurements of projectile motion in this region. One such technique is described in this report.		

At the Ballistic Research Laboratory (BRL) an M101 Howitzer was modified by cutting off the M2A2 tube at a point equivalent to 30.5 cm of projectile travel. This shortened tube, mounted in its breech mechanism, was attached well forward on the bottom carriage so that muzzle pressure would not damage the recoil mechanism, which continues to be utilized in its normal way. Thus, a recoiling launcher is available that will permit firing the entire range of 105-mm Howitzer ammunition components at full pressure and acceleration loads with a velocity reduction of about 60 percent due to the short projectile travel. In addition to the lower launch velocity which facilitates recovery of the instrumented projectile, the short tube length has the further advantage of allowing ready access to the protruding nose of the projectile for hardwire, telemetry, or photographic instrumentation measurements as required. In the work to be discussed here, hardwire linkage to projectile-borne accelerometers will be emphasized.

A description of the howitzer modification, instrumented projectile, data acquisition, and reduction is presented. Projectile motion measurements made using the 105-mm, HE, M1 projectile at the Zones 1, 5, and 7 levels are examined.

TABLE OF CONTENTS

	Page
LIST OF ILLUSTRATIONS.....	5
I. INTRODUCTION.....	7
II. TEST WEAPON.....	9
III. TEST PROJECTILE.....	12
IV. TEST AMMUNITION COMPONENTS.....	14
V. DATA ACQUISITION AND PROCESSING.....	14
VI. RESULTS.....	18
A. ZONE 1 SERIES.....	20
B. ZONE 5 SERIES.....	20
C. ZONE 7 SERIES.....	20
VII. CONCLUSIONS.....	29
ACKNOWLEDGMENTS.....	32
REFERENCES.....	32
DISTRIBUTION LIST.....	33

LIST OF ILLUSTRATIONS

<u>Figure</u>	<u>Page</u>
1. Schematic Diagram Showing Sectioning of M2A2 Tube.....	10
2. Modified M2A2 Tube Mounted in M101, Towed System.....	11
3. Modified Projectile and Components.....	12
4. Modified Lifting Plug Components.....	13
5. Exploded, Disassembled View of Modified Lifting Plug.....	13
6. Experimental Setup.....	15
7. Circuit Diagrams for Data Acquisition.....	17
8. Typical Experimental and Calculated Data for Zone 1 Firings (Round 5, B24).....	21
9. Resistive Pressure versus Travel for Round 1(T20), Zone 1.....	22
10. Resistive Pressure versus Travel for Round 2(B21), Zone 1.....	22
11. Resistive Pressure versus Travel for Round 3(B22), Zone 1.....	23
12. Resistive Pressure versus Travel for Round 4(B23), Zone 1.....	23
13. Resistive Pressure versus Travel for Round 5(B24), Zone 1.....	24
14. Resistive Pressure versus Travel for Round 6(B25), Zone 1.....	24
15. Typical Experimental and Calculated Data for Zone 5 Firings (Round 3, T15).....	25
16. Resistive Pressure versus Travel for Round 1(T13), Zone 5.....	26
17. Resistive Pressure versus Travel for Round 2(T14), Zone 5.....	26
18. Resistive Pressure versus Travel for Round 3(T15), Zone 5.....	27
19. Resistive Pressure versus Travel for Round 4(B39), Zone 5.....	27
20. Typical Experimental and Calculated Data for Zone 7 Firings (Round 2, B18).....	28
21. Resistive Pressure versus Travel for Round 1(T10), Zone 7.....	30
22. Resistive Pressure versus Travel for Round 2(B18), Zone 7.....	30
23. Resistive Pressure versus Travel for Round 3(B19), Zone 7.....	31
24. Resistive Pressure versus Travel for Round 4(B40), Zone 7.....	31

I. INTRODUCTION

One very important function of the Interior Ballistics Division of the BRL is to provide simulations of the interior ballistic performance of weapons^{1,2}. With knowledge of the performance of a known system, the performance of a slightly modified system can be simulated. This method of "ballistic similitude" has been used successfully in the past and generally provides projectile displacement, velocity, and acceleration, together with pressure data, all as a function of time, and to an accuracy that is satisfactory in most cases.

With the advent of more sophisticated projectile payloads, more complexity to propelling charge design, and newer and more exotic propellant compositions, there exists a need to refine these ballistic simulations. In the past, the use of closed-bomb burning rates and a best estimate of projectile resistance-to-motion were manipulated until satisfactory simulations were achieved; future models will require experimentally-determined inputs. Thus, there is a need to quantify resistance to projectile motion, or as we will identify it here, resistive pressure. With a measurement of the projectile linear acceleration as a function of time and with an accompanying measurement of the gas pressure acting as the forcing function on the projectile, a quantification of the resistive pressure can be made. The force balance equations for determining this resistive pressure are determined from Newton's second law of motion, as shown in Equation 1.

$$F = m \cdot a \quad (1)$$

where F = Force acting on the projectile
 m = Mass of the projectile
and a = Acceleration of the projectile.

The forces acting on the projectile in a gun firing are given by

$$F = (P_b - P_f)A \quad (2)$$

where P_b = Pressure acting on base of the projectile

P_f = Engraving and resistive pressure

and A = Cross-sectional area of the bore;

therefore, $F = m \cdot a = (P_b - P_f)A$ and $m = \frac{W}{g}$

$$\text{or } P_f = P_b - \left(\frac{W}{g} \cdot \frac{a}{A}\right) \quad (3)$$

¹P. G. Baer and J. M. Frankle, "The Simulation of Interior Ballistic Performance of Guns by Digital Computer Program," Ballistic Research Laboratories Report No. 1183, December 1962.

²J. M. Frankle, "Interior Ballistics of High-Velocity Guns, Experimental Program-Phase I," Ballistic Research Laboratories Memorandum Report No. 1879, November 1967.

where w = Projectile weight
and g = Acceleration due to gravity.

From the LaGrangian correction, base pressure (P_b) can be reasonably calculated from the measured breech pressure (P) by the expression,

$$P_b = \frac{P}{1 + \frac{c}{2w}} \quad (4)$$

where c = Propellant weight. In all our tests, the pressure gage in the chamber adapter was used for calculating P_b .

The measured, onboard acceleration calculated from combining Equations 3 and 4 is given by

$$a = \frac{g \cdot P \cdot A}{w(1 + \frac{c}{2w})} - \frac{g \cdot P_f \cdot A}{w} \quad (5)$$

Assuming no engraving and frictional losses ($P_f = 0$), calculated no-loss acceleration (a'), as shown in Equation 6, must always be larger than onboard measured acceleration; otherwise the accelerometer is inaccurate.

$$a' = \frac{g \cdot P \cdot A}{w(1 + \frac{c}{2w})} \quad (6)$$

Fundamental to the development of apparatus for taking measurements cited above are cost, ease of operation, and versatility. We conceived of a short-length howitzer with just enough in-bore travel to permit measurement of maximum chamber pressure and projectile motion during engraving and early travel over the total spectrum of standard ammunition charge increments used. Previous investigators^{3,4,5} have used a variety of techniques including our preferred technique of hardwire coupling to the projectile. Thus, the method is not new, but our variation is unique and innovative. We elected to use the modified howitzer for the following reasons:

- Reduced gun tube length decreases muzzle velocity by 60 percent at the top zone, making projectile recovery easier, if required. This facilitates retrieval of projectile-borne instrumentation.

³J.W. Evans, "In-Bore Measurement of Projectile Acceleration and Base Pressure Using an S-Band Telemetry System," Ballistic Research Laboratories Memorandum Report No. 2562, December 1975.

⁴W.P. Morrow, "A Hardwire Technique for Extracting Data from a Projectile During In-Bore Environments," Harry Diamond Laboratories, May 1972.

⁵W.D. Craig, "The Development of a "Hard-Wire" Technique for Obtaining In-Bore Data," NWL Technical Report TR-3060, November 1973.

- As designed, the short length of the gun barrel allows the nose of the projectile to protrude from the gun barrel when the projectile is seated. Since it is easily accessible, it makes the instrumentation links easier to accomplish.
- To keep instrumentation simple, we elected to use a hardwire technique, directly coupling the transducer to the recording system. This is not new but the reduced tube length allowed the use of a simplified method for accomplishing this. Telemetry could just as readily be used, but would be more expensive.
- The short-barreled howitzer eliminates the need for expensive, wire-collecting scoops because of the abbreviated travel. Other experimenters have used such scoops with success over the first several feet of travel in a howitzer.

II. TEST WEAPON

The modified 105-mm, M2A2 Howitzer tube used for examining projectile performance during early motion and the method for attaching the tube to the recoil mechanism in the M101 Towed System were conceived at BRL. The actual design and fabrication were accomplished by personnel at the Ordnance Engineering Section, Material Testing Directorate, Test and Evaluation Command, Aberdeen Proving Ground, MD.

The howitzer was modified so that the recoil mechanism, breech ring and block, and the short howitzer tube could be assembled and fired with recoil occurring in the normal way. Modifications were also necessary to insure that the muzzle position of the short howitzer tube would approximate that of the unmodified tube. If the short howitzer tube had been placed in the unmodified system, the muzzle position would have been between the recoil cylinders. The high muzzle gas pressure and temperature released into this section of the recoil mount would likely cause serious damage to either the cylinders or related mechanisms.

The modification was accomplished by sectioning the M2A2 Cannon tube as shown in the sketch in Figure 1. The tube was cut into three parts as seen in the top view, and reassembled as the modified tube shown schematically in the bottom view of the figure. Section B was threaded to permit it to be attached to the carriage at the forward hoop. An adapter, D, welded to the B section, permitted the shortened howitzer tube, A, to be fixed to the carriage and recoil mechanism. The remaining section, C, was discarded. With the cannon assembled in this fashion, it would be impossible to load the projectile and cartridge case. Therefore, Section B had the rifling removed and the inside diameter expanded to allow free passage of the projectile and cartridge case into the breech. Section A was further modified by machining a pressure gage port 38 cm from the Rear Face of the Tube (RFT). Strain patches were cemented to the outside surface of the howitzer tube at positions located 38.4, 41.5, 46.0, and 62.5 cm from the RFT to measure axial and hoop strain, if required. Four views showing the mechanical modification to the M2A2 Howitzer tube are included as Figure 2.

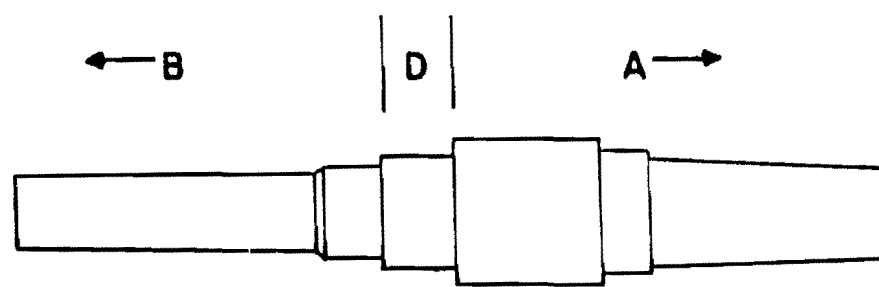
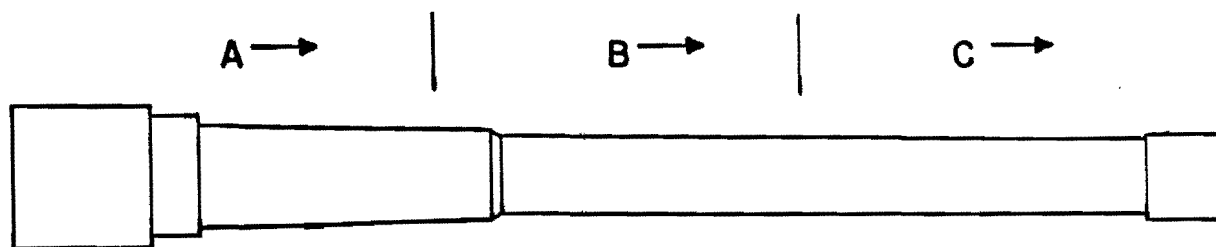


Figure 1. Schematic Diagram Showing Sectioning of M2A2 Tube.



Figure 2. Modified M2A2 Tube Mounted in M101, Towed System.

III. TEST PROJECTILE

The 105-mm, HE, M1 projectile was used for testing the hardwire instrumentation linkage. All projectiles were modified to accept a PCB, Piezotronics, Inc., accelerometer mounted in the base of the shell casing (Figure 3). A 5/32-inch (0.06-cm) hole was drilled in the base of the shell and tapped for a 10-32 UNF-2A thread. This hole was also spotfaced to a 1.3-cm diameter on the inner surface. To protect the projectile against intrusion of the propellant gases, the hole was subsequently welded shut leaving sufficient threads exposed on the interior of the projectile to mount the accelerometer. Additional protection to the accelerometer was provided by a steel cap inserted to isolate the transducer from the effects of the wax fill during setback.



Figure 3. Modified Projectile and Components

The fuze cavity for this 105-mm HE, M1 is threaded with standard 2-12 UNS threads used to accept most of the standard fuzes in the artillery projectile inventory. Larger projectiles, such as the 155-mm and 203-mm sizes, are shipped with the fuze cavity sealed with a lifting plug (Ordnance Corps Dwg 74-14-42A) for ease in handling the heavier weight shell. By machining off the ring, these lifting plugs provide an inexpensive, ready-made closure that can be used in hardwire data acquisition from the 105-mm, HE, M1 Projectile. A cross-sectional view of a modified lifting plug is shown in the sketch of Figure 4. The output from the accelerometer (not shown) is fed via a multi-stranded wire through the center array of components in the modified lifting plug. Note that the wire is looped and tied to a soldering lug in the base of the plug to provide an anchor and to prevent pulling the lead free of the accelerometer during tension loads applied in subsequent set-up and handling. To provide the proper circuit continuity in this single-lead arrangement, a copper-clad, fiberglass disc is cemented with epoxy to the outside, flat, machined surface of the lifting plug, the surface that normally would consist of the lifting ring portion of the plug. A modified brass screw and washer, and a brass and fiber washer,

arranged as shown to provide the proper insulation, make up the remaining components. The output lead, with insulation stripped off for a length of about three meters, passes through the modified brass bolt. This base lead is soft-soldered to the bolt at each end and the solder is flowed over the

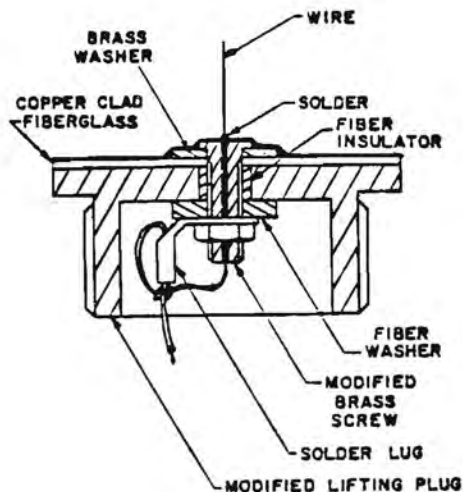


Figure 4. Modified Lifting Plug Components

copper face of the disc. The bare wire then has a contact surface as it collapses during the short, in-tube travel of the projectile. The circuit is completed through the gun tube and projectile metallic rotating band. An assembled plug and an exploded, disassembled view of the modified plug showing the various components and their orientation is shown in Figure 5.

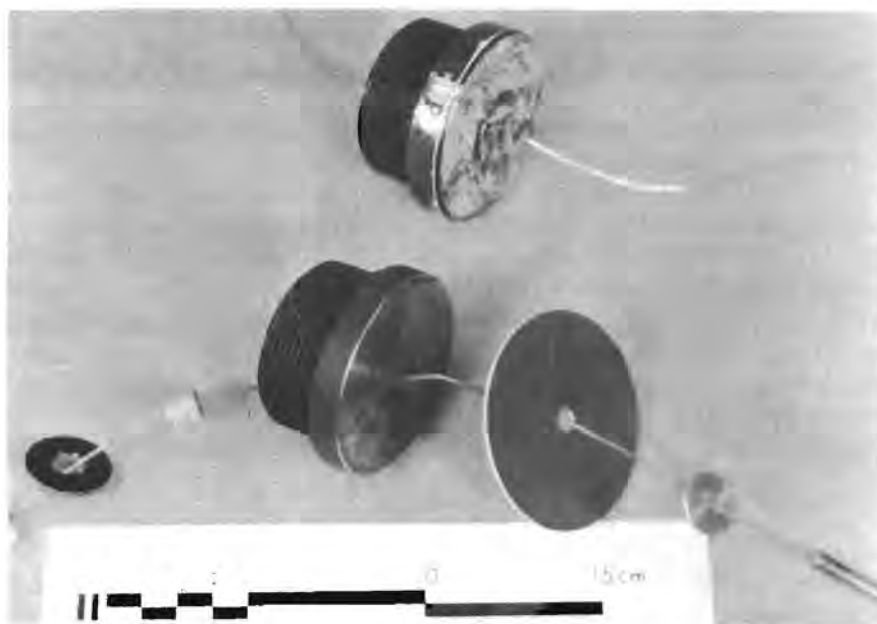


Figure 5. Exploded, Disassembled View of Modified Lifting Plug

IV. TEST AMMUNITION COMPONENTS

The 105-mm, Howitzer, M2A2 uses the M14 series cartridge cases. For the test setup used here, the M14 brass case was utilized. To minimize orientation problems with aligning a pressure-port access hole in the cartridge case, the cases were cut back 11.4 cm. The cases were also drilled and spotfaced at the base to accept a strain-type pressure transducer⁶. Experience has shown that the brass case has a longer life and affords better obturation when shortened than does the M14B1, steel case, in tests of this type.

The M28B2 Primer is a standard component for use with the M67 Propelling Charge. Early testing with this percussion primer gave ignition variability that was incompatible with our Ballistic Data Acquisition System (BALDAS). The cause of the variability was primarily due to the solenoid-actuated lanyard used to activate the firing lock. To overcome this, a modified version of the M28B2 was used. The percussion element was replaced with an electrically activated initiator that allowed the primer to be triggered with far more consistency insofar as our data recording equipment was concerned. The use of this initiator does not change the propelling charge behavior.

For all firings in this program, the M67 propelling charge was used. All ammunition components were maintained between 21-24°C for a period of at least 24 hours prior to testing.

The sketch in Figure 6 shows the relative position of the ammunition and instrumentation components, with the projectile seated in the origin-of-rifling of the shortened tube. The field experimental setup in the modified cannon with the signal lead held in position is shown in the photograph in the bottom view of the same figure.

V. DATA ACQUISITION AND PROCESSING

A PCB Piezotronics, Inc., high-shock accelerometer (Model 305A) was used for the acceleration measurements. This device contains a very small seismic mass preloaded against a quartz element by a thin-walled sleeve. This transducer also contains a p-channel, MOSFET, source follower that functions as an impedance converter. This arrangement provides the transducer with a nominal, 100-ohm, output impedance. This transducer was selected for this low-impedance characteristic to help eliminate cable length, cable contamination, and humidity problems that generally plague high-impedance devices. The relatively high output level also improved the signal-to-noise ratio. Current requirement for this device is 2 milliamperes at a quiescent voltage of 11 volts. The output signal is AC-coupled from the power lead, requiring only a two-wire transmission line to

⁶E.V. Clarke, Jr. and R.W. Deas, "Methods for Installing the IBL Miniature Pressure Gage," Ballistic Research Laboratories Technical Note No. 1662, August 1967.

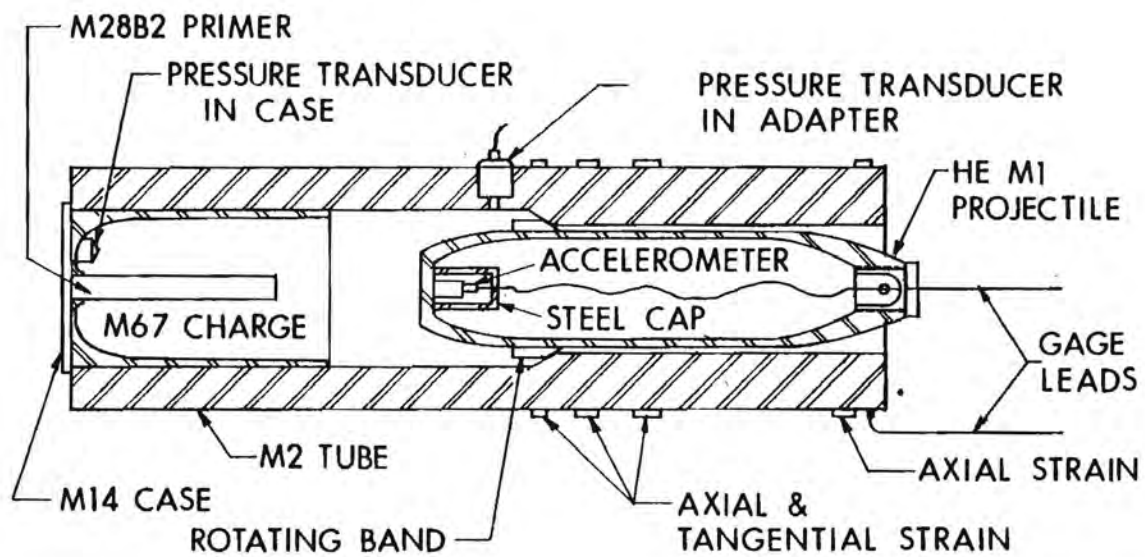


Figure 6. Experimental Setup.

the signal conditioning instrumentation.

Since it was planned to manipulate the data from the accelerometer with that of the pressure transducer to measure the resistive pressure, the analog data paths were made as identical as possible. To help accomplish this, a PCB Model 109A Pressure Transducer was used since it also has a similar, built-in source follower circuit. The rise times of the two transducers were of the same order of magnitude but had different discharge time constants. This was not a problem since the event time was short and both transducers could follow it.

In order to keep the data reduction process compatible with existing hardware and software, a standard format was used. This format places five linear calibration steps of fifty-milliseconds duration just prior to the analog event. This analog calibration and data are digitized in real time and stored in the core memory of a PDP 11/45 mini-computer accommodating from two to sixteen channels of data in the 24K storage. Analog-to-digital conversion rates vary between four and twenty-two microseconds per sample, depending on the number of channels handled. The analog signals are simultaneously recorded on FM, magnetic tape, providing a source for post-firing digitization if required. Since the data are permanently stored on digital magnetic tape, the data can be recalled for further processing at any time.

A simplified diagram of the transducer and signal conditioning circuit is shown in the top view of Figure 7. The transducer crystal is shunted with a capacitor that adjusts the sensitivity to the transducer. The resistor biases the gate and removes any long-term, thermal-induced charge on the crystal element. The transducer is connected to the piezotron input of a dual-mode amplifier (Kistler Model 504E4). This charge amplifier has a built-in constant current source that biases the transducer. A parallel input circuit, with an external calibration capacitor, is connected to the staircase calibration source. The amplitude of the maximum calibration step is selected to be equal to the maximum expected output to be seen during the event. The dual-mode amplifier is adjusted using the range selector switch and sensitivity potentiometer to the desired level. Since this amplifier inverts the signal, an inverting data amplifier is needed to establish the proper polarity and off-set to the signal required by the recording system.

The analog system to measure the resistive pressure is shown in the bottom view of Figure 7. This technique results in the analog differencing of the accelerometer and pressure transducer output signals with a system that is properly adjusted, calibrated, and scaled. The maximum calibration voltage for the pressure transducer is obtained from the relationship:

$$V_p = P/K_p \quad (7)$$

where

V_p = Top calibration step voltage (volts)

P = Maximum expected pressure (MPa)

K_p = Transducer sensitivity (MPa/volt)

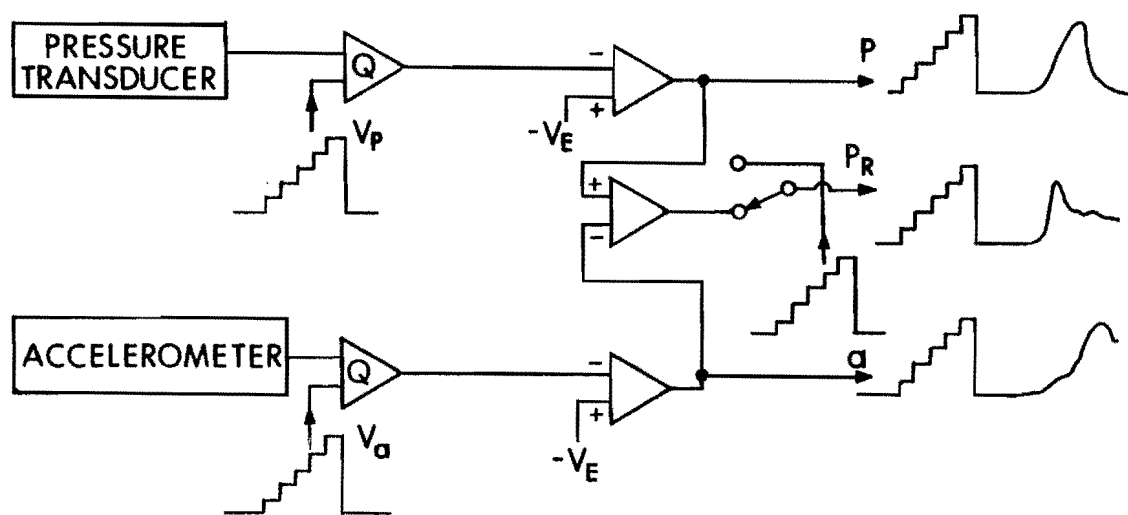
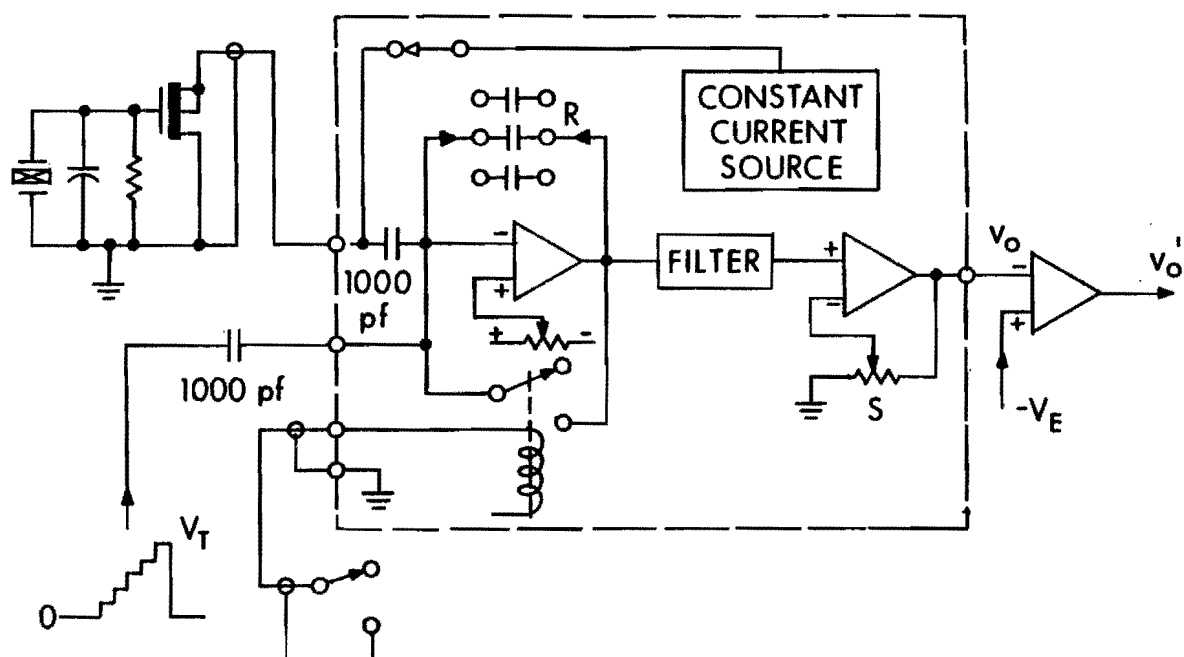


Figure 7. Circuit Diagrams for Data Acquisition.

The maximum accelerometer calibration voltage is selected to scale the acceleration term in the force balance equation (Equation 1) so it will have the same units and same magnitude as the pressure term. This is done by first assuming that the system is frictionless and then calculating the maximum possible acceleration for the expected applied base pressure using Equation 6.

The top step voltage for the accelerometer calibration output is likewise selected from the relationship

$$V_a = a/K_a \quad (8)$$

where,

V_a = Top calibration stop voltage (volts)

a = Maximum expected acceleration (Kilo g's)

K_a = Accelerometer sensitivity (Kilo g's per volt)

The outputs of the two dual-mode amplifiers (Q) are then adjusted for compatibility with the recording device and the analog voltages of the two staircase calibrations are adjusted for the same amplitude. The two output signals are then differenced using a differential amplifier. This output is interrupted during the calibration cycle for insertion of the voltage calibration staircase. The resistive pressure calibration is obtained by dividing the pressure calibration by the gain of the differential amplifier.

VI. RESULTS

The short-barrelled howitzer has been successfully test-fired at three different rates-of-loading using the Zones 1, 5, and 7 levels of the M67 Propelling Charge. No adverse effects to the recoil mechanism have been observed due to the blast effects of the higher-than-normal "muzzle" pressures that develop as the result of the greatly-reduced tube length. Recoil displacement with the reduced tube mass has not exceeded 56 cm. The use of the modified lifting plug as an inexpensive method of obtaining a hardwire data link has also proven highly successful and inexpensive. Lower velocity launch and the ability to recover the transducers for reuse has also been achieved by firing the projectiles into a sand-filled, steel trough five meters forward of the howitzer.

All pertinent data for each of the firings are shown on Table 1. Chamber pressure, onboard acceleration, and doppler muzzle velocity were experimentally determined; base pressure was computed from chamber pressure using the LaGrangian correction for pressure gradient. Peak engraving pressure was taken from the plots of "Calculated Resistive Pressure versus Displacement from Accelerometer (resistive pressure-displacement)" calculated from chamber pressure and onboard acceleration data (Figures 8-24). The "no-loss" onboard acceleration was computed from Equation 6.

TABLE 1. Projectiles with Guiding Metal Rotating Bands

Round (Code) Number	Zone	Projectile Wt. (Kg)	Chamber Pressure (MPa)	Base Pressure (MPa)	Onboard Acceler- ation (Km/s/s)	"No-Loss" Acceler- ation (Cal- culated (Km/s/s)	Peak Engraving Pressure (MPa)	Resistive ^(*2) Pressure Af- ter 20 cm of Travel (MPa)	Muzzle Velocity (m/s)
1 (T20)	1	14.9	52.1	51.6	24.9	31.3	32.5	8	123.7
2 (B21)	"	"	48.4	47.9	23.9	29.1	26.1	8	131.1
3 (B22)	"	"	50.4	49.9	27.9	30.3	24.5	4	134.7
4 (B23)	"	"	57.0	56.5	29.9	34.3	29.8	4	134.7
5 (B24)	"	"	56.3	55.6	29.9	33.7	29.8	7	137.8
6 (B25)	"	"	56.8	56.0	31.9	33.9	28.0	1 ^(*3)	134.7
Avg		14.9	53.5	52.9	28.1	32.2	28.4	5.3	132.8
Std Dev		0	3.7	3.6	3.1	2.0	2.9	2.7	4.9
1 (T13)	5	14.8	101.8	100.0	55.9	61.1	32.3	1 ^(*3)	197.5
2 (T14)	"	14.7	96.9	94.6	51.9	57.8	24.7	11	191.1
3 (T15)	"	14.5	100.0	98.2	51.9	60.4	32.3	14	197.5
4 (B39)	"	14.7	99.4	98.2	51.9	61.2	40.1	23	205.6
Avg		14.7	99.5	97.8	52.9	60.1	32.4	12.2	197.9
Std Dev		0.1	2.0	2.3	2.0	1.6	6.3	9.1	(5.9)
1 (T10)	7	14.7	230.4	222.2	101.9	136.6	68.3	57 ^(*4)	314.5
2 (B18)	"	14.8	237.6	227.4	133.7	138.9	21.3	16	303.9
3 (B19)	"	14.7	232.6	224.3	121.8	137.9	22.2	30	314.8
4 (B40)	"	15.1	246.9	236.6	120.8	141.6	25.2	25	299.3
Avg		14.8	234.8	227.6	119.6 (125.4) ^(*1)	138.8 (22.9) ^(*1)	34.2 (22.9) ^(*1)	32	308.1
Std Dev		0.2	10.3	6.4	13.1 (7.2)	2.1	22.7 (2.0)	17.6	7.8

(*1) Average and standard deviation for four and three rounds. Round 1(T10) had an abnormally low peak acceleration compared to peak pressure that affects calculated peak engraving pressure.

(*2) Average resistive pressure was taken after 20 cm of travel which was close to muzzle exit and prior to loss of signal.

(*3) Rapidly changing (both increasing or decreasing) downtube resistive pressure.

(*4) Value taken at 15 cm of travel since data beyond this point was lost.

A. Zone 1 Series

Round-by-Round data for the Zone 1 series are shown in Table 1. The plotted data for Round 5(B24) in Figure 8 illustrate pressure and acceleration data typical of all six rounds in the series. Both the chamber and base pressure versus time plots (upper right and left) show an increased pressure decay when the projectile exits the short tube, an event corroborated by loss of signal from the onboard accelerometer (center plot). Initial projectile motion and band engraving occurred between 8 and 15 ms when the accelerometer output was responding in a wavering fashion. After engraving there was a rapid increase in gage output as the projectile began to accelerate down the tube. As the projectile velocity approached its maximum, there was a decrease in acceleration until the projectile exited the tube wherein the accelerometer signal was lost. Onboard acceleration ranged from 23.9 to 31.9 km/s/s and was, in all cases, less than that calculated for a "no-loss" system.

Calculated resistive pressure as shown in Figure 8 was plotted both as a function of time (bottom left) and as a function of displacement (bottom right) obtained by integrating twice the accelerometer-time curve. The well-defined resistive pressure-displacement profile typical of all rounds in the Zone 1 series (Figures 9 thru 14) exhibits a large engraving pressure over the first 2-3 cm of travel (approximately 1-3 times the rotating band width) followed by a greatly reduced frictional pressure over the downtube travel.

B. Zone 5 Series

Round-by-Round data for the Zone 5 Series are shown in Table 1. The plots of Figure 15 for Round 3(T15) are typical of pressure and acceleration data for all four rounds in this series. As in the Zone 1 Series, there is rapid pressure decay after projectile exit because the short tube length combined with the relatively high muzzle pressures leads to a fast tube emptying process. Initial projectile motion and engraving occurred between 10 and 12.5 ms for this round as indicated by a rapid rise in accelerometer output followed by a dip in the output. There was not the wavering output as noted in the Zone 1 Series. After engraving, the profile was similar in most cases to Series 1. Onboard acceleration ranged from 51.9 to 55.9 km/s/s.

The well-defined resistive pressure-displacement profiles having a large engraving pressure followed by a much smaller resistive pressure were typical, in varying degrees, of all rounds in this series (Figures 16 thru 19). Round 4(B39) had a large momentary loss of accelerometer transmission which calculated into a large peak in the downtube resistive pressure profile that was not typical of the experimentally-observed data.

C. Zone 7 Series

Round-by-Round data for the Zone 7 Series are shown in Table 1. The plotted data for Round 2(B18) in Figure 20 show typical pressure and acceleration data for three of the four rounds in this series. As in the Zone 1 and 5 series, pressure decays rapidly after the projectile exits the short tube. Initial projectile motion and engraving occurred between 8 and

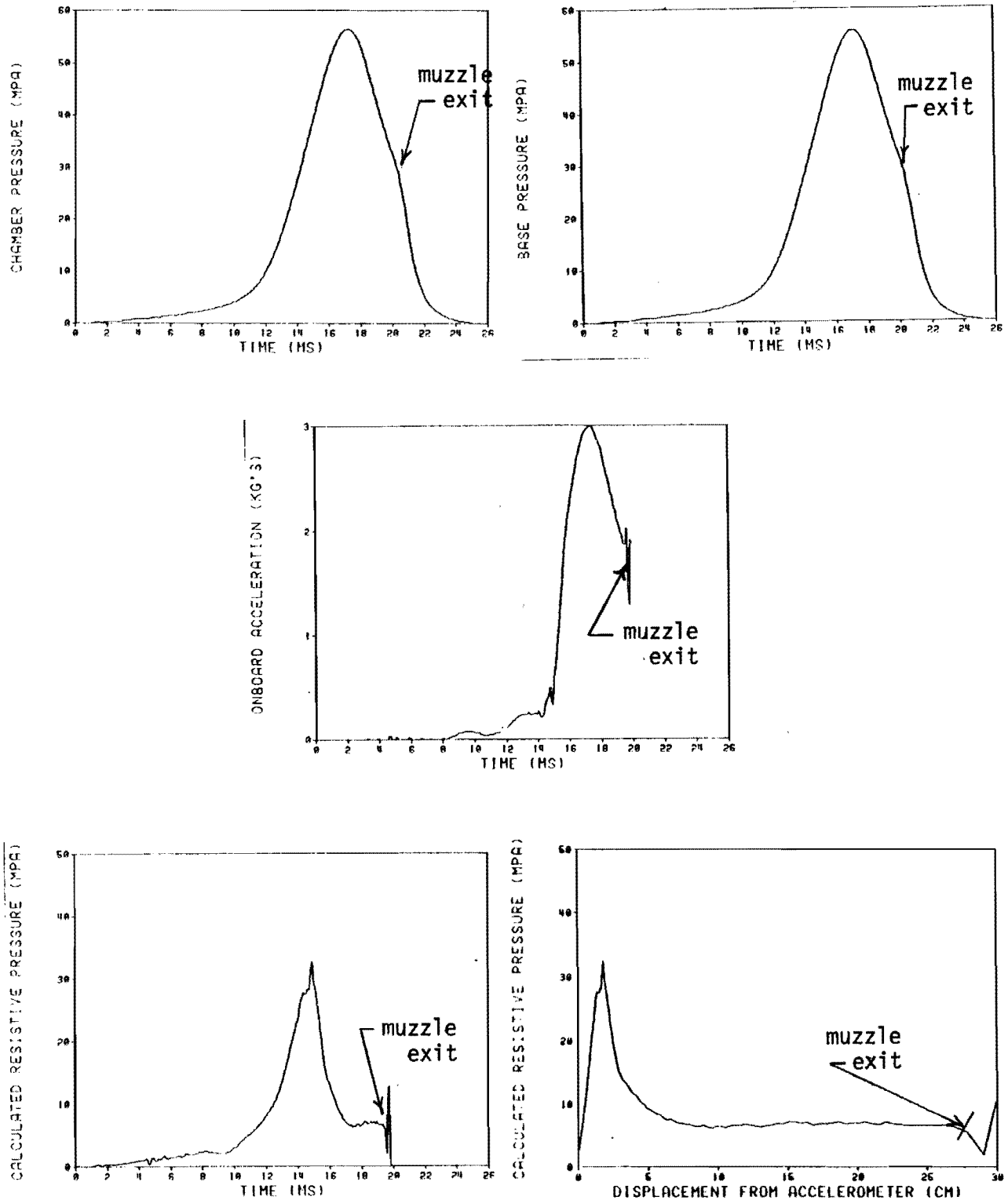


Figure 8. Typical Experimental and Calculated Data for Zone 1 Firings (Round 5, B24).

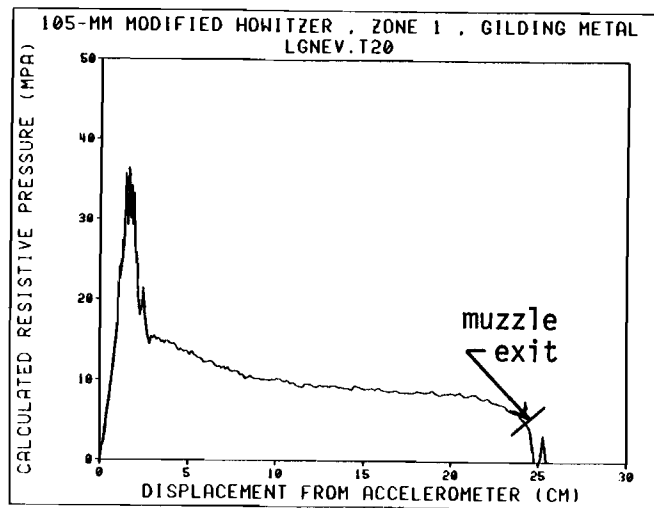


Figure 9. Resistive Pressure versus Travel for Round 1(T20), Zone 1.

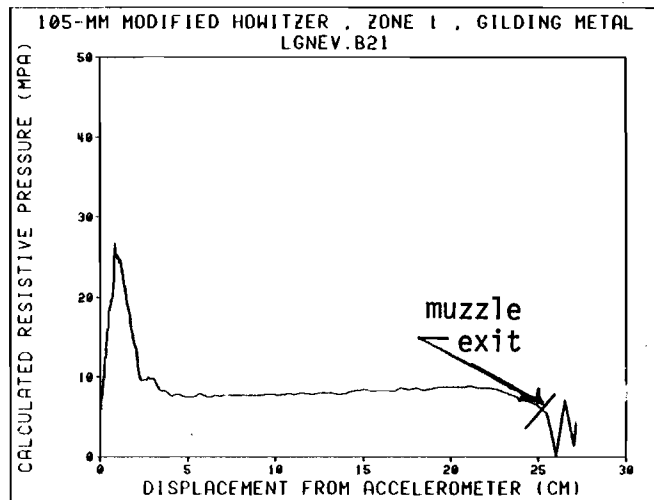


Figure 10. Resistive Pressure versus Travel for Round 2(B21), Zone 1.

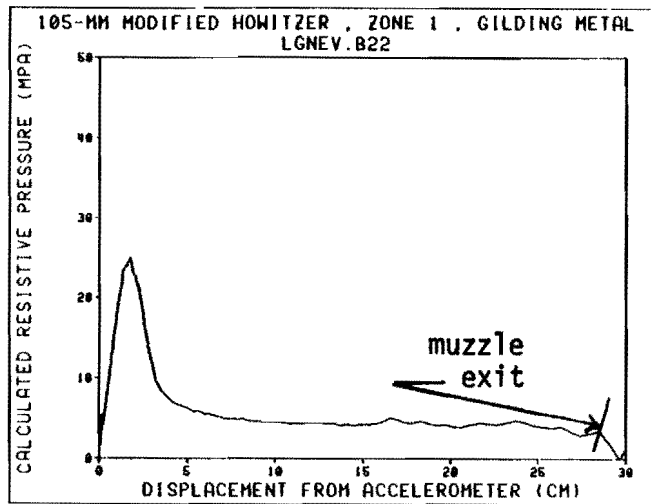


Figure 11. Resistive Pressure versus Travel for Round 3(B22), Zone 1.

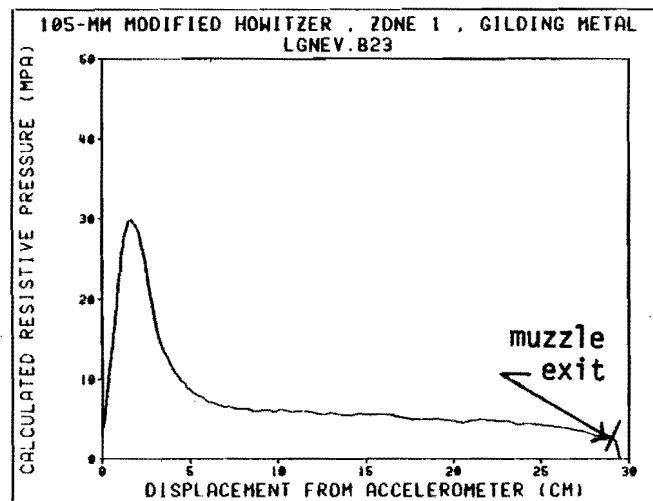


Figure 12. Resistive Pressure versus Travel for Round 4(B23), Zone 1.

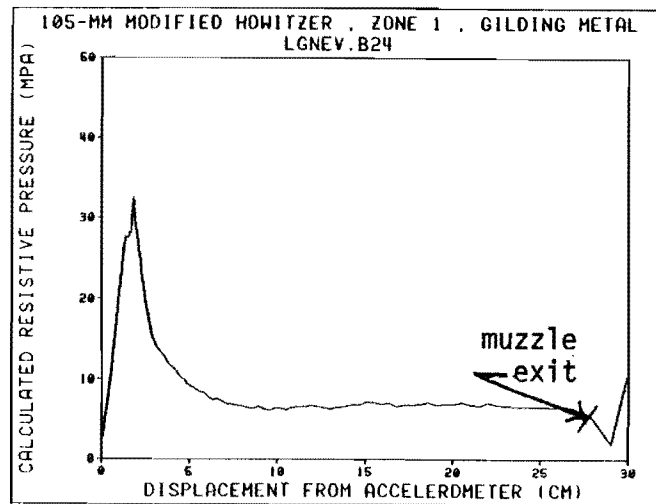


Figure 13. Resistive Pressure versus Travel for Round 5(B24), Zone 1.

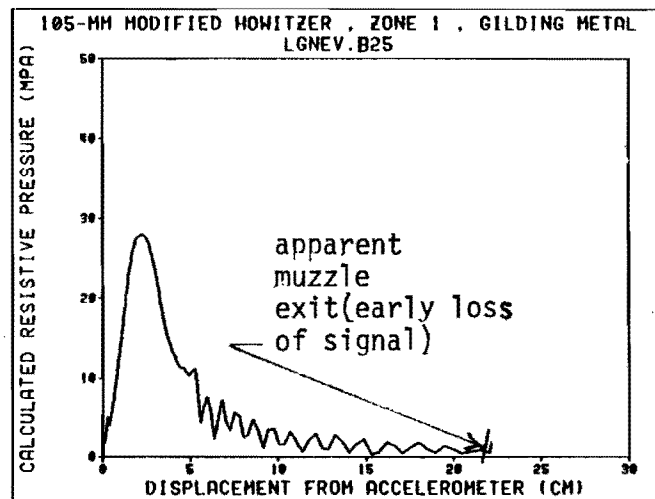


Figure 14. Resistive Pressure versus Travel for Round 6(B25), Zone 1.

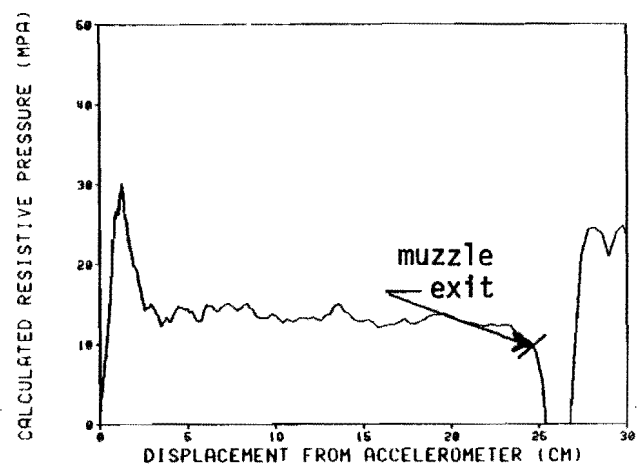
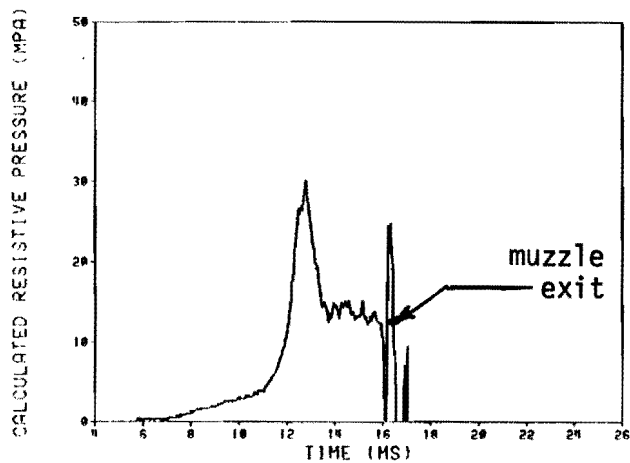
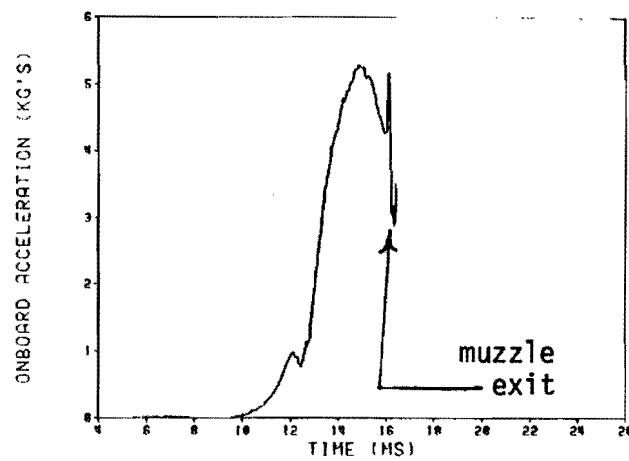
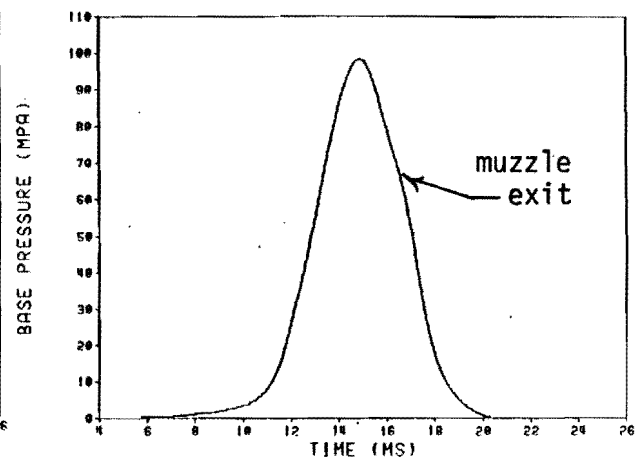
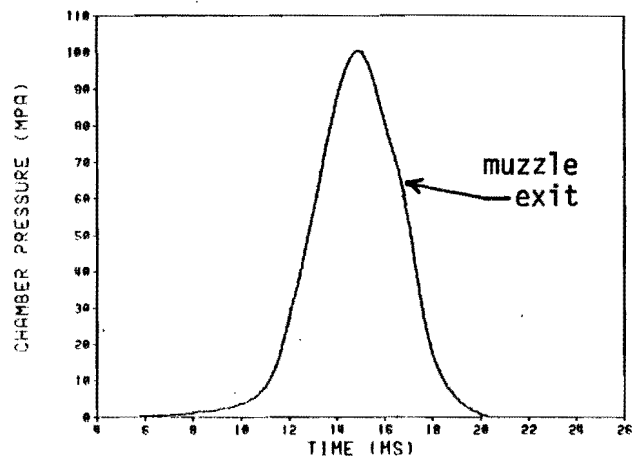


Figure 15. Typical Experimental and Calculated Data for Zone 5 Firings (Round 3, T15).

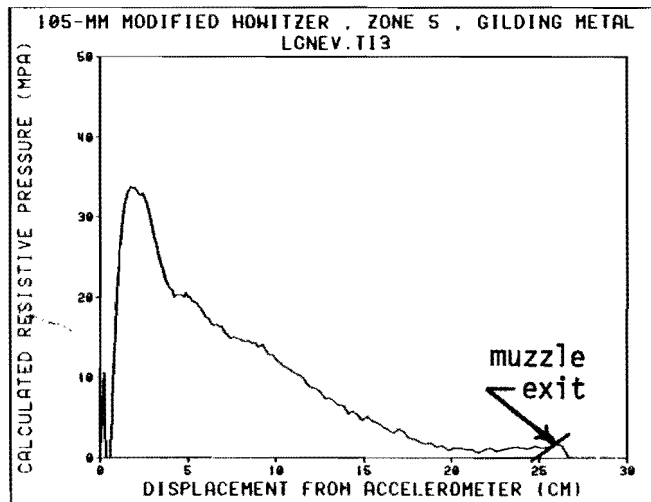


Figure 16. Resistive Pressure versus Travel for Round 1(T13), Zone 5.

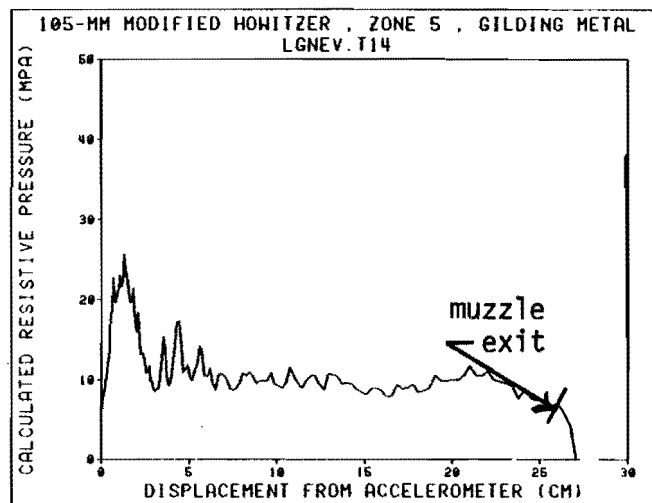


Figure 17. Resistive Pressure versus Travel for Round 2(T14), Zone 5.

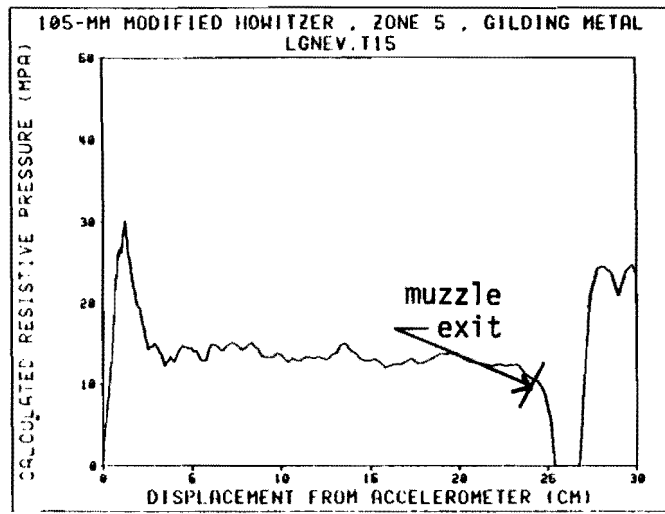


Figure 18. Resistive Pressure versus Travel for Round 3(T15), Zone 5.

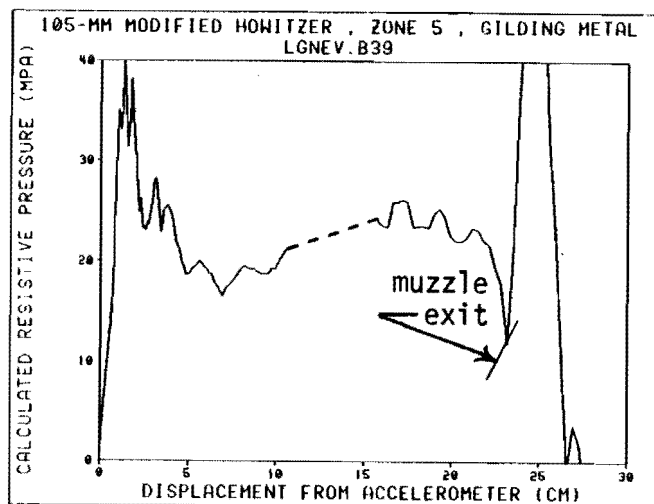


Figure 19. Resistive Pressure versus Travel for Round 4(B39), Zone 5.

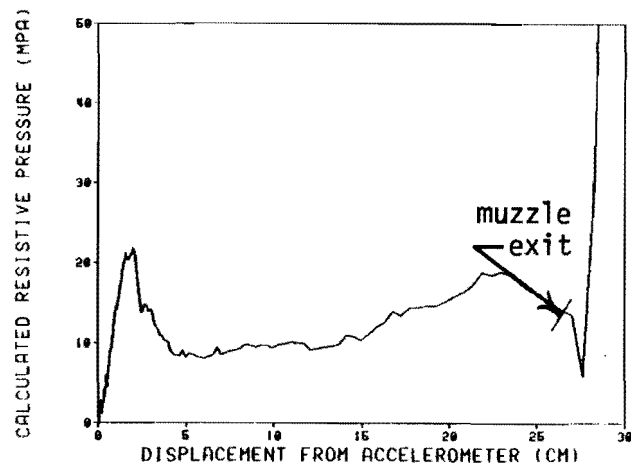
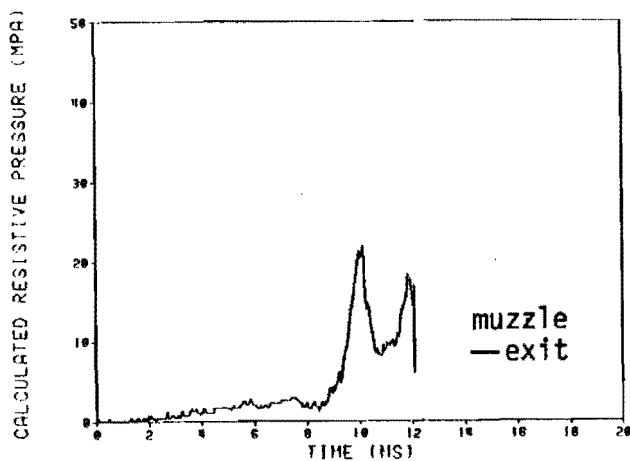
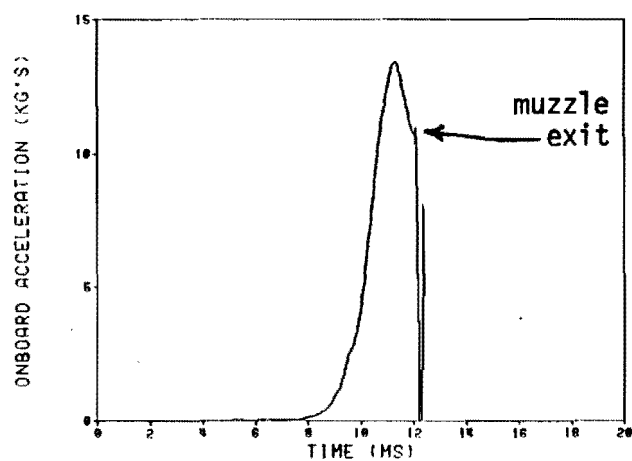
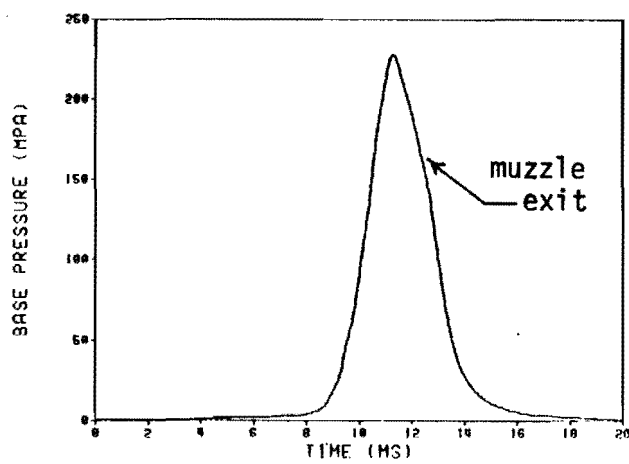
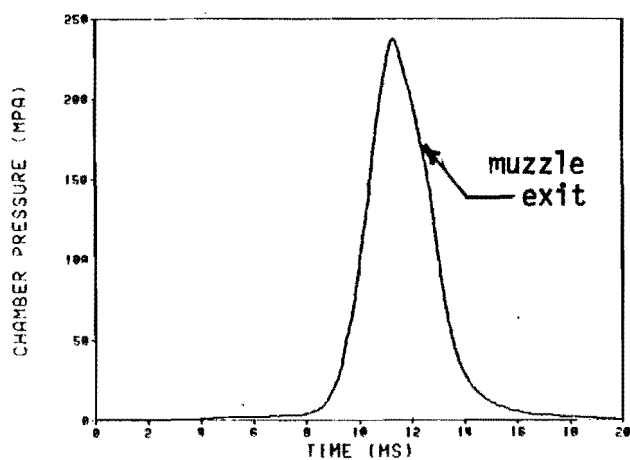


Figure 20. Typical Experimental and Calculated Data for Zone 7 Firings (Round 2, B18).

9.5 ms for this round. A slight change in the slope of the acceleration-time curve at 9.5 ms is the only indication of the engraving since rapid burning of propellant quickly accelerates the projectile, almost masking the engraving process. Peak acceleration varied from 101.9 to 133.7 km/s/s. In Table 1, an average and standard deviation are given for both four and three rounds. Round 1(T10) is excluded in the 3-round comparison since the 101.9 km/s/s seems to be well below that expected in comparison to its chamber pressure level. In all cases, the calculated "no-loss" acceleration was larger than the experimentally-measured values.

As shown in Figures 21 thru 24, no round in the Zone 7 Series had the well-defined profiles previously indicated for Series 1 and 5. In three of the four cases (Round 2(T10) being the anomaly), there was a reasonably good engraving pressure. As the engraving pressure decreased, it quickly reached a minimum level after which it began to increase with increasing travel rather than maintaining the lower level as was the case in the Zone 1- and 5- series firings. This increasing resistive pressure with travel occurred, in varying degrees, for all four rounds in the series. The resistive pressure-displacement profiles for Round 1(T10) is highly suspect since the peak acceleration value for the onboard accelerometer was much lower than would be expected for its corresponding chamber pressure.

VII. CONCLUSIONS

A simple and inexpensive technique for the instrumentation and monitoring of an accelerometer onboard a 105-mm howitzer projectile has been demonstrated. The technique employed in this program has direct application for work anticipated on a 155-mm, instrumented projectile fired from a short-barreled howitzer.

Onboard acceleration-time measurements taken at three rates-of-loading (Zones 1, 5, and 7) for a gilding metal-banded projectile were successful in that the onboard data was in the correct range based on peak pressure measurements in the howitzer chamber. The average peak engraving pressure for all three zones was similar being 28.4 MPa for the Zone 1 Series, 32.4 MPa for the Zone 5 Series, and 33.2 MPa for the Zone 1 Series. After omitting Round 1(T10) from the Zone 7 Series since it gave an unusually low value of peak acceleration, the peak engraving pressure drops from 34.2 MPa to 22.7 MPa.

The average downtube resistive pressure profiles for the three zones differed considerably. Both Zone 1 and Zone 5 Series dropped rapidly from their peak engraving pressure values to a consistent low level until shot ejection. For the Zone 7 Series, all rounds except Round 1(T10) which had a low peak acceleration, dropped somewhat from their peak engraving value but then began to increase with increasing travel down the tube. In two of the four rounds, the resistive pressure near the muzzle was higher than the initial engraving pressure for the round. This was surprising since we expected with increasing projectile in-tube travel, the resistive pressure profile to be always less than the peak engraving pressure.

Useful measurements of the behavior of the projectile during in-bore travel are necessary to determine the effects of this severe environment on

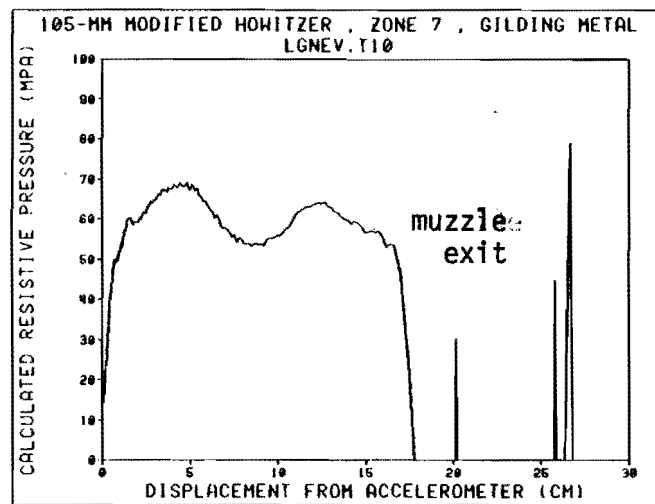


Figure 21. Resistive Pressure versus Travel for Round 1(T10), Zone 7.

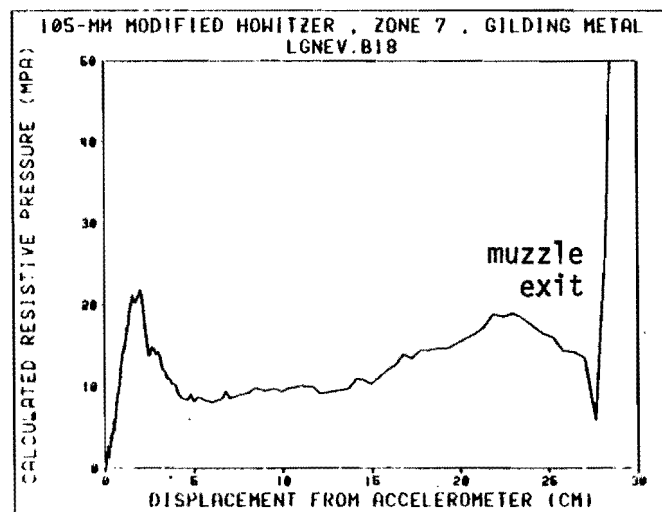


Figure 22. Resistive Pressure versus Travel for Round 2(B18), Zone 7.

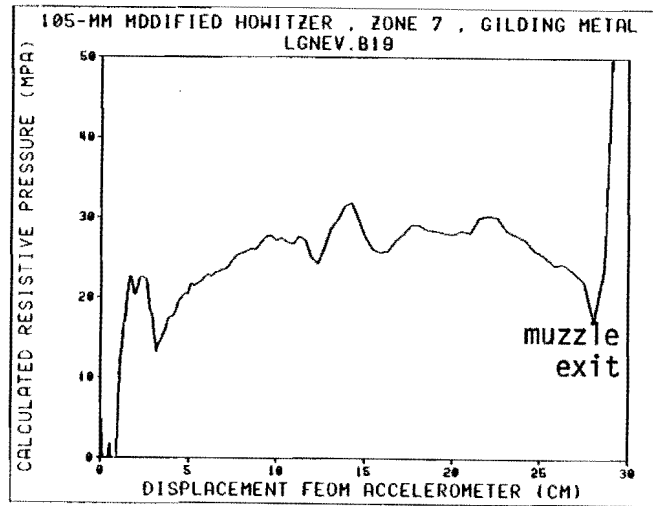


Figure 23. Resistive Pressure versus Travel for Round 3(B19), Zone 7.

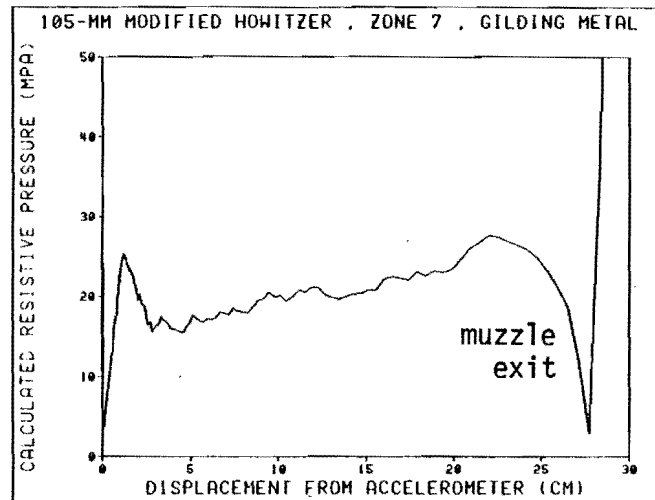


Figure 24. Resistive Pressure versus Travel for Round 4(B40), Zone 7.

the system. Refinements in the method of calibrating the accelerometers are a requirement for transmitted data to accurately reflect the dynamic conditions onboard the projectile.

ACKNOWLEDGMENT

The authors wish to express their gratitude for the assistance provided by the Interior Ballistics Division, BRL personnel involved in this work. Notable among these are J. Bowen, J. Hewitt and J. Stabile.

REFERENCES

1. P. G. Baer and J. M. Frankle, "The Simulation of Interior Ballistic Performance of Guns by Digital Computer Program," Ballistic Research Laboratories Report No. 1183, December 1962.
2. J. M. Frankle, "Interior Ballistics of High-Velocity Guns, Experimental Program-Phase I," Ballistic Research Laboratories Memorandum Report No. 1879, November 1967.
3. J. W. Evans, "In-Bore Measurement of Projectile Acceleration and Base Pressure Using an S-Band Telemetry System," Ballistic Research Laboratories Memorandum Report No. 2562, December 1975.
4. W. P. Morrow, "A Hardwire Technique for Extracting Data from a Projectile During In-Bore Environments," Harry Diamond Laboratories, May 1972.
5. W. D. Craig, "The Development of a "Hard-Wire" Technique for Obtaining In-Bore Data," NWL Technical Report TR-3060, November 1973.
6. E. V. Clarke, Jr. and R. W. Deas, "Methods for Installing the IBL-Miniature Pressure Gage," Ballistic Research Laboratories Technical Note No. 1662, August 1967.

DISTRIBUTION LIST

<u>No. Of Copies</u>	<u>Organization</u>	<u>No. Of Copies</u>	<u>Organization</u>
12	Administrator Defense Technical Info Center ATTN: DTIC-DDA Cameron Station Alexandria, VA 22314	3	Commander US Army Materiel Development and Readiness Command ATTN: DRCMD- ST DCRSF-E, Safety Office DRCDE-DW 5001 Eisenhower Avenue Alexandria, VA 22333
1	Office of the Under Secretary of Defense Research & Engineering ATTN: R. Thorkildsen Washington, DC 20301	14	Commander US Army Armament R&D Command ATTN: DRDAR-TSS DRDAR-TDC D. Gyorog DRDAR-LCA K. Russell A. Moss J. Lannon A. Beardell D. Downs S. Einstein L. Schlosberg S. Westley S. Bernstein P. Kemmey C. Heyman Dover, NJ 07801
1	HQDA/SAUS-OR, D. Hardison Washington, DC 20301		
1	HQDA/DAMA-ZA Washington, DC 20310		
2	HQDA, DAMA-CSM, A. German E. Lippi Washington, DC 20310		
1	HQDA/SARDA Washington, DC 20310		
1	Commandant US Army War College ATTN: Library-FF229 Carlisle Barracks, PA 17013	9	US Army Armament R&D Command ATTN: DRDAR-SCA, L. Stiefel B. Brodman DRDAR-LCB-I, D. Spring DRDAR-LCE, R. Walker DRDAR-LCU-CT E. Barrieres R. Davitt DRDAR-LCU-CV C.Mandala E. Moore DRDAR-LCM-E S. Kaplowitz Dover, NJ 07801
1	Ballistic Missile Defense Advanced Technology Center P. O. Box 1500 Huntsville, AL 35804		
1	Chairman DOD Explosives Safety Board Room 856-C Hoffman Bldg. 1 2461 Eisenhower Avenue Alexandria, VA 22331		

DISTRIBUTION LIST

<u>No. Of Copies</u>	<u>Organization</u>	<u>No. Of Copies</u>	<u>Organization</u>
5	Commander US Army Armament R&D Command ATTN: DRDAR-QAR, J. Rutkowski G. Allen J. Donner P. Serao D. Adams Dover, NJ 07801	5	Commander US Army Armament Materiel Readiness Command ATTN: DRDAR-LEP-L, Tech Lib DRSAR-LC, L. Ambrosini DRSAR-IRC, G. Cowan DRSAR-LEM, W. Fortune R. Zastrow Rock Island, IL 61299
5	Project Manager Cannon Artillery Weapons System ATTN: DRCPM-CAWS F. Menke DRCPM-CAWS-WS H. Noble DRCPM-CAWS-SI M. Fisette DRCPM-CAWS-AM R. DeKleine H. Hassmann Dover, NJ 07801	1	Commander US Army Watervliet Arsenal ATTN: SARWV-RD, R. Thierry Watervliet, NY 12189
		1	Director US Army ARRADCOM Benet Weapons Laboratory ATTN: DRDAR-LCB-TL Watervliet, NY 12189
		1	Commander US Army Aviation Research and Development Command ATTN: DRDAV-E 4300 Goodfellow Blvd. St. Louis, MO 63120
3	Project Manager Munitions Production Base Modernization and Expansion ATTN: DRCPM-PMB, J. Ziegler M. Lohr A. Siklosi Dover, NJ 07801	1	Commander US Army TSARCOM 4300 Goodfellow Blvd St. Louis, MO 63120
3	Project Manager Tank Main Armament System ATTN: DRCPM-TMA, D. Appling DRCPM-TMA-105 DRCPM-TMA-120 Dover, NJ 07801	1	Director US Army Air Mobility Research And Development Laboratory Ames Research Center Moffett Field, CA 94035
4	Commander US Army Armament R&D Command ATTN: DRDAR-LCW-A M. Salsbury DRDAR-LCS DRDAR-LCU, A. Moss DRDAR-LC, J. Frasier Dover, NJ 07801		

DISTRIBUTION LIST

<u>No. Of Copies</u>	<u>Organization</u>	<u>No. Of Copies</u>	<u>Organization</u>
1	Commander US Army Communications Research and Development Command ATTN: DRDCO-PPA-SA Fort Monmouth, NJ 07703	1	Project Manager Improved TOW Vehicle ATTN: DRCPM-ITV US Army Tank Automotive Research & Development Command Warren, MI 48090
1	Commander US Army Electronics Research and Development Command Technical Support Activity ATTN: DELSD-L Fort Monmouth, NJ 07703	2	Program Manager M1 Abrams Tank System ATTN: DRCPM-GMC-SA, J. Roossien Warren, MI 48090
1	Commander US Army Harry Diamond Lab. ATTN: DELHD-TA-L 2800 Powder Mill Road Adelphi, MD 20783	1	Project Manager Fighting Vehicle Systems ATTN: DRCPM-FVS Warren, MI 48090
2	Commander US Army Missile Command ATTN: DRSMI-R DRSMI-YDL Redstone Arsenal, AL 35898	1	Director US Army TRADOC Systems Analysis Activity ATTN: ATAA-SL, Tech Lib White Sands Missile Range, NM 88002
1	Commander US Army Natick Research and Development Command ATTN: DRDNA-DT, D. Sieling Natick, MA 01762	1	Project Manager M-60 Tank Development ATTN: DRCPM-M60TD Warren, MI 48090
1	Commander US Army Tank Automotive Research and Development Command ATTN: DRDTA-UL Warren, MI 48090	1	Commander US Army Training & Doctrine Command ATTN: ATCD-M Fort Monroe, VA 23651
1	US Army Tank Automotive Materiel Readiness Command ATTN: DRSTA-CG Warren, MI 48090	2	Commander US Army Materials and Mechanics Research Center ATTN: DRXMR-ATL Tech Library Watertown, MA 02172

DISTRIBUTION LIST

<u>No. Of Copies</u>	<u>Organization</u>	<u>No. Of Copies</u>	<u>Organization</u>
1	Commander US Army Research Office ATTN: Tech Library P. O. Box 12211 Research Triangle Park, NC 27709	1	Commander US Army Foreign Science & Technology Center ATTN: DRXST-MC-3 220 Seventh Street, NE Charlottesville, VA 22901
1	Commander US Army Mobility Equipment Research & Development Command ATTN: DRDME-WC Fort Belvoir, VA 22060	1	President US Army Artillery Board Ft. Sill, OK 73504
1	Commander US Army Logistics Mgmt Ctr Defense Logistics Studies Fort Lee, VA 23801	2	Commandant US Army Field Artillery School ATTN: ATSF-CO-MW, B. Willis Ft. Sill, OK 73503
2	Commandant US Army Infantry School ATTN: Infantry Agency Fort Benning, GA 31905	3	Commandant US Army Armor School ATTN: ATZK-CD-MS/M. Falkovitch/Armor Agency Fort Knox, KY 40120
1	US Army Armor & Engineer Board ATTN: STEBB-AD-S Fort Knox, KY 40121	1	Chief of Naval Materiel Department of the Navy ATTN: J. Amlie Washington, DC 20360
1	Commandant US Army Aviation School ATTN: Aviation Agency Fort Rucker, AL 36360	1	Chief Naval Research ATTN: Code 473, R. S. Miller 800 N. Quincy Street Arlington, VA 22217
1	Commandant Command and General Staff College Fort Leavenworth, KS 66027	2	Commander Naval Sea Systems Command ATTN: SEA-62R, J. W. Murrin R. Beauregard Washington, DC 20362
1	Commandant US Army Special Warfare School ATTN: Rev & Tng Lit Div Fort Bragg, NC 28307	1	Commander Naval Air Systems Command ATTN: NAIR-954-Tech Lib Washington, DC 20360
1	Commandant US Army Engineer School ATTN: ATSE-CD Ft. Belvoir, VA 22060		

DISTRIBUTION LIST

<u>No. Of Copies</u>	<u>Organization</u>	<u>No. Of Copies</u>	<u>Organization</u>
1	Strategic Systems Project Office Dept. of the Navy Room 901 ATTN: J. F. Kincaid Washington, DC 20376	4	Commander Naval Weapons Center ATTN: Code 388, R. L. Derr C. F. Price T. Boggs Info. Sci. Div. China Lake, CA 93555
1	Assistant Secretary of the Navy (R, E, and S) ATTN: R. Reichenbach Room 5E787 Pentagon Bldg. Washington, DC 20350	2	Superintendent Naval Postgraduate School Dept. of Mechanical Engineering ATTN: A. E. Fuhs Code 1424 Library Monterey, CA 93940
1	Naval Research Lab Tech Library Washington, DC 20375	6	Commander Naval Ordnance Station ATTN: P. L. Stang C. Smith S. Mitchell C. Christensen D. Brooks Tech Library Indian Head, MD 20640
5	Commander Naval Surface Weapons Center ATTN: Code G33, J. L. East D. McClure W. Burrell J. Johndrow Code DX-21 Tech Lib Dahlgren, VA 22448	1	AFSC Andrews AFB Washington, DC 20331
2	Commander US Naval Surface Weapons Center ATTN: J. P. Consaga C. Gotzmer Indian Head, MD 20640	1	Program Manager AFOSR Directorate of Aerospace Sciences ATTN: L. H. Caveny Bolling AFB, DC 20332
4	Commander Naval Surface Weapons Center ATTN: S. Jacobs/Code 240 Code 730 K. Kim/Code R-13 R. Bernecker Silver Spring, MD 20910	6	AFRPL (DYSC) ATTN: D. George J. N. Levine B. Goshgarian D. Thrasher N. Vander Hyde Tech Library Edwards AFB, CA 93523
2	Commanding Officer Naval Underwater Systems Center Energy Conversion Dept. ATTN: CODE 5B331, R. S. Lazar Tech Lib Newport, RI 02840		

DISTRIBUTION LIST

<u>No. Of Copies</u>	<u>Organization</u>	<u>No. Of Copies</u>	<u>Organization</u>
1	AFFTC ATTN: SSD-Tech Lib Edwards AFB, CA 93523	1	AVCO Everett Rsch Lab Div ATTN: D. Stickler 2385 Revere Beach Parkway Everett, MA 02149
1	AFATL ATTN: DLYV Eglin AFB, FL 32542	2	Calspan Corporation ATTN: E. B. Fisher Tech Library P. O. Box 400 Buffalo, NY 14225
1	AFATL/DLDL ATTN: O. K. Heiney Eglin AFB, FL 32542	1	Foster Miller Associates, ATTN: A. Erickson 135 Second Avenue Waltham, MA 02154
1	ADTC ATTN: DLODL Tech Lib Eglin AFB, FL 32542	1	Hercules, Inc. Bacchus Works ATTN: K. P. McCarty Magna, UT 84044
1	AFFDL ATTN: TST-Lib Wright-Patterson AFB, OH 45433	1	General Applied Sciences Lab ATTN: J. Erdos Merrick & Stewart Avenues Westbury Long Island, NY 11590
1	NASA HQ 600 Independence Avenue, SW ATTN: Code JM6, Tech Lib. Washington, DC 20546	1	General Electric Company Armament Systems Dept. ATTN: M. J. Bulman, Room 1311 Lakeside Avenue Burlington, VT 05412
1	NASA/Lyndon B. Johnson Space Center ATTN: NHS-22, Library Section Houston, TX 77058	1	Hercules Powder Co. Allegheny Ballistics Laboratory ATTN: R. B. Miller P. O. Box 210 Cumberland, MD 21501
1	Aerodyne Research, Inc. Bedford Research Park ATTN: V. Yousefian Bedford, MA 01730	1	Hercules, Inc Bacchus Works ATTN: K. P. McCarty P. O. Box 98 Magna, UT 84044
1	Aerojet Solid Propulsion Co. ATTN: P. Micheli Sacramento, CA 95813		
1	Atlantic Research Corporation ATTN: M. K. King 5390 Cheorokee Avenue Alexandria, VA 22314		

DISTRIBUTION LIST

<u>No. Of Copies</u>	<u>Organization</u>	<u>No. Of Copies</u>	<u>Organization</u>
1	Hercules, Inc. Eglin Operations AFATL DLDL ATTN: R. L. Simmons Eglin AFB, FL 32542	2	Rockwell International Rocketdyne Division ATTN: BA08 J. E. Flanagan J. Grey 6633 Canoga Avenue Canoga Park, CA 91304
1	IITRI ATTN: M. J. Klein 10 W. 35th Street Chicago, IL 60615	1	Science Applications, INC. ATTN: R. B. Edelman 23146 Cumorah Crest Woodland Hills, CA 91364
2	Lawrence Livermore Laboratory ATTN: M. S. L-355, A. Buckingham M. Finger P. O. Box 808 Livermore, CA 94550	1	Scientific Research Assoc., Inc. ATTN: H. McDonald P. O. Box 498 Glastonbury, CT 06033
1	Olin Corporation Badger Army Ammunition Plant ATTN: R. J. Thiede Baraboo, WI 53913	1	Shock Hydrodynamics, Inc. ATTN: W. H. Andersen 4710-16 Vineland Avenue North Hollywood, CA 91602
1	Olin Corporation Smokeless Powder Operations ATTN: R. L. Cook P. O. Box 222 ST. Marks, FL 32355	3	Thiokol Corporation Huntsville Division ATTN: D. Flanigan R. Glick Tech Library Huntsville, AL 35807
1	Paul Gough Associates, Inc. ATTN: P. S. Gough P. O. Box 1614 Portsmouth, NH 03801	2	Thiokol Corporation Wasatch Division ATTN: J. Peterson Tech Library P. O. Box 524 Brigham City, UT 84302
1	Physics International Company 2700 Merced Street Leandro, CA 94577		
1	Princeton Combustion Research Lab., Inc. ATTN: M. Summerfield 1041 US Highway One North Princeton, NJ 08540	2	Thiokol Corporation Elkton Division ATTN: R. Biddle Tech Lib. P. O. Box 241 Elkton, MD 21921
1	Pulsepower Systems, Inc. ATTN: L. C. Elmore 815 American Street San Carlos, CA 94070		

DISTRIBUTION LIST

<u>No. Of Copies</u>	<u>Organization</u>	<u>No. Of Copies</u>	<u>Organization</u>
2	United Technologies Chemical Systems Division ATTN: R. Brown Tech Library P. O. Box 358 Sunnyvale, CA 94086	1	University of Massachusetts Dept. of Mechanical Engineering ATTN: K. Jakus Amherst, MA 01002
1	Universal Propulsion Company ATTN: H. J. McSpadden Black Canyon Stage 1, Box 1140 Phoenix, AZ 85029	1	University of Minnesota Dept. of Mechanical Engineering ATTN: E. Fletcher Minneapolis, MN 55455
1	Southwest Research Institute 8500 Culebra Road San Antonio, TX 78228	1	Case Western Reserve University Division of Aerospace Sciences ATTN: J. Tien Cleveland, OH 44135
1	Battelle Memorial Institute ATTN: Tech Library 505 King avenue Columbus, OH 43201	3	Georgia Institute of Tech School of Aerospace Eng. ATTN: B. T. Zinn E. Price W. C. Strahle Atlanta, GA 30332
1	Brigham Young University Dept. of Chemical Engineering ATTN: Dr. M. Beckstead Provo, UT 84601	1	Institute of Gas Technology ATTN: D. Gidaspow 3424 S. State Street Chicago, IL 60616
1	California Institute of Tech 204 Karman Lab Main Stop 301-46 ATTN: F. E. C. Culick 1201 E. California Street Pasadena, CA 91125	1	Johns Hopkins University Applied Physics Laboratory Chemical Propulsion Information Agency ATTN: T. Christian Johns Hopkins Road Laurel, MD 20707
1	Director Jet Propulsion Laboratory 4800 Oak Grove Drive Pasadena, CA 91103	1	Massachusetts Institute of Tech Dept of Mechanical Engineering ATTN: T. Toong Cambridge, MA 02139
1	University of Illinois Dept. of Mech Eng ATTN: H. Krier 144 MEB, 1206 W. Green St. Urbana, IL 61801		

DISTRIBUTION LIST

<u>No. Of Copies</u>	<u>Organization</u>	<u>No. Of Copies</u>	<u>Organization</u>
1	Pennsylvania State University Applied Research Lab ATTN: G. M. Faeth P. O. Box 30 State College, PA 16801	1	University of Southern California Mechanical Engineering Dept. ATTN: OHE200, M. Gerstein Los Angeles, CA 90007
1	Pennsylvania State University Dept. Of Mechanical Engineering ATTN: K. Kuo University Park, PA 16802	2	University of Utah Dept. of Chemical Engineering ATTN: A. Baer G. Flandro Salt Lake City, UT 84112
1	Purdue University School of Mechanical Engineering ATTN: J. R. Osborn TSPC Chaffee Hall West Lafayette, IN 47906	1	Washington State University Dept. of Mechanical Engineering ATTN: C. T. Crowe Pullman, WA 99164
1	Rensselaer Polytechnic Inst. Department of Mathematics Troy, NY 12181	<u>Aberdeen Proving Ground</u>	
1	Rutgers University Dept. of Mechanical and Aerospace Engineering ATTN: S. Temkin University Heights Campus New Brunswick, NJ 08903	Dir, USAMSAA ATTN: DRXSY-D DRXSY-MP, H. Cohen Cdr, USATECOM ATTN: DRSTE-TO-F STEAP-MT, S. Walton G. Rice D. Lacey C. Herud	
1	SRI International Propulsion Sciences Division ATTN: Tech Library 333 Ravenswood Avenue Menlo Park, CA 94025	Dir, HEL ATTN: J. Weisz Dir, USACSL, Bldg. E3516, EA ATTN: DRDAR-CLB-PA	
1	Stevens Institute of Technology Davidson Laboratory ATTN: R. McAlevy, III Hoboken, NJ 07030		
2	Los Alamos Scientific Lab ATTN: T. B. Butler, MS B216 M. Division, B. Craig P. O. Box 1663 Los Alamos, NM 87545		